

## Chaotic Rydberg Atoms with Broken Time-Reversal Symmetry

Krzysztof Sacha,<sup>1</sup> Jakub Zakrzewski,<sup>1</sup> and Dominique Delande<sup>2</sup>

<sup>1</sup>*Instytut Fizyki imienia Mariana Smoluchowskiego, Uniwersytet Jagielloński, ulica Reymonta 4, PL-30-059 Kraków, Poland*

<sup>2</sup>*Laboratoire Kastler-Brossel, Tour 12, Étage 1, Université Pierre et Marie Curie, 4 Place Jussieu, 75005 Paris, France*

(Received 29 June 1999)

The dynamics of Rydberg states of atomic hydrogen perturbed simultaneously by a static electric field and a resonant microwave field of elliptical polarization is analyzed in the quantum perturbative limit of small amplitudes. For some configurations, the secular motion (i.e., evolution in time of the elliptical electronic trajectory) may be classically predominantly chaotic. By changing the orientation of the static field with respect to the polarization of the microwave field, one can modify the global symmetries of the system and break any generalized time-reversal invariance. This has a dramatic effect on the statistical properties of the energy levels.

PACS numbers: 05.45.Mt, 32.80.Rm, 42.50.Hz

One of the fundamental questions in quantum chaos is the correspondence between the classical dynamics of a given Hamiltonian dynamical system and the statistical properties of the energy spectrum of its quantum counterpart [1]. Universal fluctuation properties occur when the corresponding classical system is either integrable or chaotic. The spectral fluctuations for a classically integrable system obey Poissonian statistics [2]. In another extreme, i.e., ergodicity, the statistical properties of quantum spectra can be modeled by ensembles of random matrices, namely, with a GOE (Gaussian orthogonal ensemble) in the case of time-reversal invariant (or more generally, any other antiunitary invariance) systems or with GUE (Gaussian unitary ensemble) in the absence of such a symmetry [1]. For a generic Hamiltonian system, where typically chaotic and regular motions coexist, the fluctuations are expected to interpolate between these two limiting universal cases [3–5]. While experimental observations of transition to chaos have been made for time-reversal invariant systems, the system studied below allows for the breaking of the antiunitary symmetry. As far as we know, this is the first experimentally realizable example of such a situation in a quantum system (for wave chaos experiments, see [6]).

Perturbed Coulomb systems are ideally suited for studies of a manifestation of classical chaos in quantum mechanics [7] both theoretically and *experimentally*. A hydrogenlike atom in a uniform magnetic field reveals a smooth transition to chaos [7] with increasing magnetic field. Similarly the motion of the electron in an atom driven by electromagnetic radiation undergoes a smooth transition to chaos with increasing field amplitude [7]. On the other hand, the anisotropic Kepler problem (modeling defects in semiconductors) becomes chaotic as soon as the effective mass becomes direction dependent [8]. Different reactions to perturbations are just a manifestation of the inapplicability of the Kolmogorov-Arnold-Moser theorem [8] to a highly degenerate Coulomb problem.

In this Letter, we consider the perturbation of the hydrogen (H) atom by very weak static electric and resonant

microwave fields. Classically, such fields may produce chaotic dynamics in the secular motion of the atom (i.e., in the motion of the electronic ellipse). In the quantum mechanical language, states coming from a given manifold with fixed principal quantum number  $n_0$  may significantly mix only with each other. Thus, we may observe an “intra-manifold” chaos, in which a finite number (possibly  $n_0^2$ ) of quantum levels are involved (provided the coupling to the continuum is negligible). Intra-manifold chaos requires the strong mixing of at least 2 different degrees of freedom, here the total angular momentum and its  $z$  component.

The simplest system where such a behavior has been expected is a hydrogen atom perturbed by uniform static electric and magnetic fields of arbitrary mutual orientation [9,10]. At lowest nonvanishing order (small fields) the perturbation leaves a constant of the motion. By including second order terms, signatures of chaos have been observed in the quantum spectrum [9,10]. The necessary fields are, however, big and higher order terms—neglected in this approach—of comparable importance. Moreover, the high electric field leads then to fast field ionization which will blur the effects discussed. The situation discussed below does not suffer from this deficiency. Moreover it allows us to study the influence of an antiunitary symmetry breaking on the level statistics.

We consider a realistic three-dimensional H atom placed in a static electric field and driven by elliptically polarized microwaves. We define the  $z$  axis as perpendicular to the plane of polarization of the microwave field. The Hamiltonian of the system in atomic units, neglecting relativistic effects, assuming infinite mass of the nucleus, and employing dipole approximation reads

$$H = \frac{\mathbf{p}^2}{2} - \frac{1}{r} + F(x \cos \omega t + \alpha y \sin \omega t) + \mathbf{E} \cdot \mathbf{r}, \quad (1)$$

where  $F$ ,  $\alpha$ , and  $\omega$  stand, respectively, for the amplitude, degree of elliptical polarization, and frequency of microwave field while  $\mathbf{E}$  denotes the static electric field vector. The resonant driving of Rydberg states with principal quantum number  $n_0$  occurs when the atom is

illuminated by a microwave field of frequency fulfilling  $\omega_0 = \omega/\omega_K = m$ , where  $m$  is an integer number and  $\omega_K = 1/n_0^3$  is the frequency of the unperturbed Kepler motion.

Because of time periodicity, the Hamiltonian has a series of quasienergy levels, corresponding to the energy levels of the atomic system dressed by the microwave photons. To calculate these quasienergy levels, we employ a quantum perturbation method, whose details will be given elsewhere. In short, the method defines an effective Hamiltonian [11] in a given manifold, which takes into account the *direct* coupling between the levels due to the presence of the static electric field and the *indirect* coupling through all levels of other manifolds, i.e., process of absorption and emission of microwave photons. The *direct* couplings gives a first order contribution of the static field while the *indirect* ones contribute at second order of the microwave field. The effective Hamiltonian inside a given hydrogenic manifold is thus the sum of a term proportional to  $E$  and a term proportional to  $F^2$ . For arbitrary mutual orientations of the two fields, the two terms have incompatible symmetry properties and, when having comparable magnitudes, induce a global chaotic behavior. The resulting matrix of dimension  $n_0^2$  is diagonalized by standard routines. The method has been validated in the limiting case of combined weak static and linearly polarized microwave fields [12].

The semiclassical approach is an extension of the methods used in our previous studies [13,14]. It relies on quantization of the fast orbital motion of the electron keeping fixed the electronic ellipse. In the resonant case, this motion is pendulumlike. Taking the appropriate limiting case (valid for very weak fields) of the corresponding Mathieu equation solution [15] yields the effective Hamiltonian for the secular motion of the electronic ellipse, which is the classical equivalent of the effective quantum Hamiltonian discussed above. It is expressed as

$$H_{\text{sec}} = \frac{F_0^2}{3m^2} \Gamma_{m,0}^2 + \frac{E_0}{n_0^2} \gamma, \quad (2)$$

where the constant  $-1/2n_0^2$  term was omitted ( $H_{\text{sec}}$  denotes the shift from the unperturbed energy level of the atom), and

$$\begin{aligned} \gamma = & -\frac{3}{2} \left[ \cos\varphi \sin\theta \left( \cos\phi \cos\psi - \frac{M_0}{L_0} \sin\phi \sin\psi \right) \right. \\ & + \sin\varphi \sin\theta \left( \sin\phi \cos\psi + \frac{M_0}{L_0} \cos\phi \sin\psi \right) \\ & \left. + \cos\theta \sqrt{1 - \frac{M_0^2}{L_0^2} \sin^2\psi} \right] \sqrt{1 - L_0^2}. \quad (3) \end{aligned}$$

$F_0 = n_0^4 F$ ,  $E_0 = n_0^4 E$ ,  $L_0 = L/n_0$ , and  $M_0 = M/n_0$  are the scaled microwave and static electric field amplitudes, the scaled angular momentum, and the projection of the

angular momentum on the  $z$  axis, respectively. The  $\psi$  and  $\phi$  angles are canonically conjugate variables to the  $L_0$  and  $M_0$  momenta, respectively. Orientation of the static field vector with respect to the  $z$  axis is given by the spherical angles  $\varphi$  and  $\theta$ . The expression for  $\gamma$  looks complicated, but it is actually nothing but the component of the average atomic dipole on the static field axis. The explicit expression for  $\Gamma_{m,0} = \Gamma_m/n_0^2$  is given in [16], Eq. (2.16).

To calculate the quasienergies of the system, one should perform quantization of the secular motion determined by the Hamiltonian (2). It has been done in simpler situations (e.g., H atom perturbed by linearly polarized microwaves and a parallel static electric field) [13]. Then the secular motion is integrable and its quantization straightforward. The present secular problem (2 degrees of freedom) turns out to be nonintegrable.

Equation (2) has some well defined scaling properties with the field strengths  $F_0$  and  $E_0$ . Let us define the reduced microwave strength  $\mathcal{F} = F_0^2 n_0^2 / E_0 = F^2 n_0^6 / E$  and the reduced Hamiltonian

$$\mathcal{H} = H_{\text{sec}} n_0^2 / E_0 = \frac{\mathcal{F}}{3m^2} \Gamma_{m,0}^2 + \gamma. \quad (4)$$

The classical phase space structure depends only on the value of  $\mathcal{H}$  and  $\mathcal{F}$  (beside the static field vector orientation and the polarization of the microwave), but not on the detailed values of  $n_0$ ,  $E$ ,  $F$ , and the secular energy. Of course, weaker fields imply a slower secular motion, but this does not affect the structure of phase space. In the quantum mechanical picture, the energy splitting of a degenerate hydrogenic manifold also depends on absolute values of the fields, but the structure of the levels does not.

For generic orientations of the fields, all symmetry properties are broken. It is only for  $\varphi$  equal to 0 or  $\pi/2$  that the system has some antiunitary invariance, under the combination of time-reversal transformation with reflection with respect to the  $YZ$  or  $XZ$  plane; see (1). To observe the quantum signature of the breaking of the antiunitary symmetry, it is convenient to have a predominantly chaotic classical dynamics, as a transition from GOE to GUE statistics is expected. After rather extensive searches with various values of the parameters, we have found that the 2:1 resonance, i.e.,  $\omega_0 = m = 2$ , is more suitable than the principal one as it produces a more chaotic dynamics. The choice  $\theta \approx \pi/4$ ,  $\alpha = 0.4$ , and  $\mathcal{F} = 5000$  maximizes chaoticity of the system for reduced energy  $\mathcal{H}$  in the range 8.5–9.5. A Poincaré surface of section for these parameters (and  $\varphi = \pi/4$ ) is shown in Fig. 1 and displays chaos very predominantly. Moreover, the phase space structure does not change significantly if we set  $\varphi$  equal to 0 or  $\pi/2$  (for  $\varphi = 0$  the regular layer is slightly larger while for  $\varphi = \pi/2$  it disappears).

To obtain better statistics, the quantum levels were found for different orientation angles  $\varphi, \theta = \{0.2\pi, 0.25\pi, 0.3\pi\}$  and different  $n_0 = 99-101$  values,

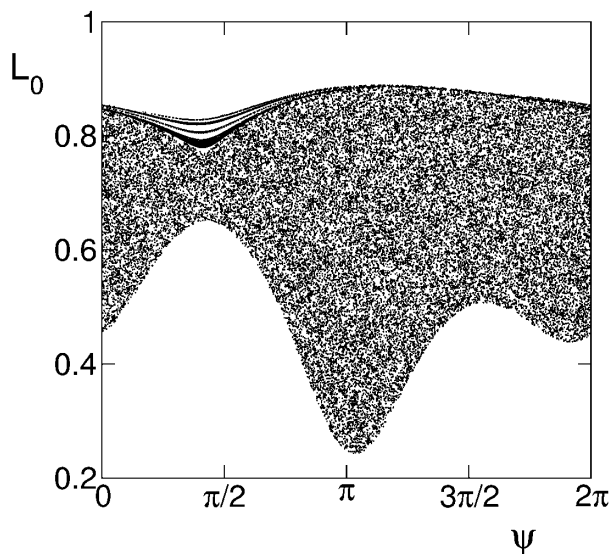


FIG. 1. Poincaré surface of section (at  $\phi = 0$ ) of the classical secular motion, Eq. (2), for  $\mathcal{H} = 8.5$ , with parameters of the fields  $\mathcal{F} = 5000$ ,  $\omega_0 = 2$  (i.e.,  $m = 2$ ),  $\alpha = 0.4$ . Orientation of the static electric field vector  $\varphi = \theta = \pi/4$ . Note that, for the parameters chosen, not the whole  $(L_0, \psi)$  space is accessible.

keeping other parameters as in Fig. 1. From each diagonalization, we took a fragment of spectrum corresponding to the quasi-energy interval 8.5–9.5 and unfolded the spectra to produce the statistical distributions.

The cumulative nearest neighbor spacing (NNS) distribution is plotted in Fig. 2 together with the similar distributions corresponding to GOE and GUE [1]. It is apparent that the calculated numerical data traces between GOE and GUE, clearly demonstrating the breaking of the antiunitary symmetry. The data do not reach the GUE behavior because the corresponding classical dynamics is not entirely ergodic. To measure the departure from the GUE distribution, one may fit different theoretical distributions. A natural choice is Berry-Robnik statistics [5] (for independent superposition of Poisson and GUE spectra) which allows one to estimate the relative measure  $q$  of the chaotic part of classical phase space. The best fit is for  $q = 0.94$  which is in agreement with Fig. 1. However, the agreement with the Berry-Robnik distribution is not perfect (see Fig. 2), which suggests that the deep semiclassical limit, required for Berry-Robnik statistics [5], is not reached yet in our data.

The statistical distribution proposed by Izrailev [4] is more appropriate. Indeed, it fits the numerical NNS distribution quite impressively (compare Fig. 2) yielding the “repulsion parameter”  $\beta = 1.47$ , roughly in the middle between the GOE ( $\beta = 1$ ) and GUE ( $\beta = 2$ ) values.

To focus on the long range correlations in the spectra, we study also the spectral rigidity, i.e.,  $\Delta_3$  statistics [1]. It gives independent information about the relative measure  $q$  of the chaotic part of phase space. For a superposition

of independent Poissonian and GUE spectra, one obtains [1,5]

$$\Delta_3(L) = \Delta_3^{\text{Poisson}}[(1 - q)L] + \Delta_3^{\text{GUE}}(qL). \quad (5)$$

Fitting Eq. (5) to the numerical spectral rigidity results in  $q = 0.94$ , which is in excellent agreement with the value of  $q$  obtained from NNS distribution. In Fig. 3, we also present the spectral rigidities obtained for antiunitary symmetry invariant cases, i.e., for  $\varphi = 0$  and  $\varphi = \pi/2$ . Their detailed analysis is left for a future publication. It is sufficient to say that, for  $\varphi = 0$ , the phase space structure is slightly more regular than the one shown in Fig. 1 and consequently the fitted parameter  $q = 0.82$  is smaller [for the antiunitary invariant problem  $\Delta_3^{\text{GUE}}$  is substituted by  $\Delta_3^{\text{GOE}}$  in Eq. (5)]. On the other hand, for  $\varphi = \pi/2$ , the classical phase space reveals more chaotic character and thus  $q = 0.95$ . Note that the saturation of  $\Delta_3$ , for all presented cases, appears for  $L \approx 40$  [2].

We have here considered small but finite field amplitudes to stay well within the applicability range of the quantum perturbation theory. We expect, however, a similar behavior for larger amplitudes. While we present

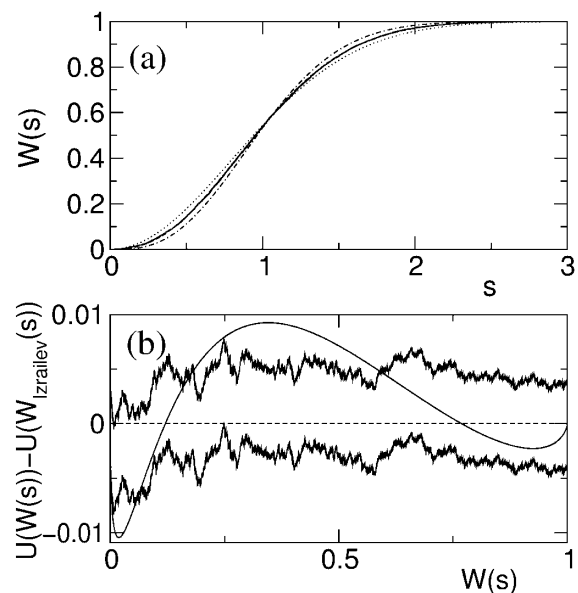


FIG. 2. Cumulative level spacing distributions  $W(s)$ . In panel (a), the solid line represents the numerical data for  $n_0 = 99-101$ ,  $\mathcal{F} = 5000$ ,  $\omega_0 = 2$ ,  $\alpha = 0.4$ , and different static electric field vector orientations  $\varphi, \theta = \{0.2\pi, 0.25\pi, 0.3\pi\}$  (there are about 6000 spacings); dashed line (hardly visible behind the solid line): the best fitting Izrailev distribution with its parameter  $\beta = 1.47$ ; dotted and dash-dotted lines: GOE and GUE distributions, respectively. Panel (b) shows a fine-scale representation of the deviation of the numerical level spacing distribution from the best fitting Izrailev distribution in terms of the  $U[W(s)] - U[W_{\text{Izrailev}}(s)]$  vs  $W(s)$ ; the transformation  $U(W) = \arccos \sqrt{1 - W}$  is used in order to have uniform statistical error over the plot [5]. The upper and lower noisy curves represent 1 standard deviation from the calculated numerical data which thus lie in the middle of the band. The solid curve is the best Berry-Robnik distribution,  $q = 0.94$ .

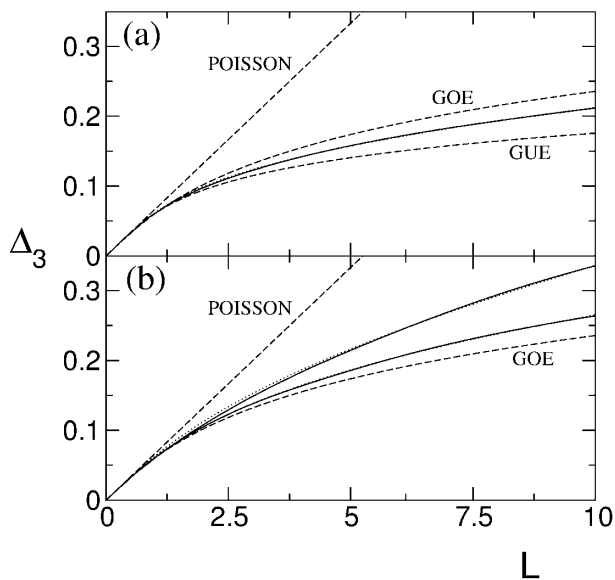


FIG. 3. Spectral rigidity  $\Delta_3$  compared with random ensemble predictions. Panel (a) shows the results for numerical data (solid line) in the broken antiunitary invariance case (with the same parameters as in Fig. 2) together with the fit of Eq. (5) (dots, barely visible behind the solid line, fitted value  $q = 0.94$ ). Dashed lines indicate Poisson, GOE, and GUE predictions as indicated in the figure. Panel (b) shows numerical data for an antiunitary invariant case with the same parameters as in Fig. 2, but for  $\varphi = 0$  and  $n_0 = 97-102$  for the upper case and  $\varphi = \pi/2$  for the lower line. The fitted values for the fraction of chaotic phase space volume are  $q = 0.82$  and  $q = 0.95$ , respectively.

numerical data for  $n_0 \approx 100$  for better statistics, a clear signature is also observed for  $n_0 \approx 50$ . There, the of independent Poissonian and GUE spectra, one obtains [1,5] of independent Poissonian and GUE spectra, one obtains [1,5] expected mean level spacing is of the order of a few MHz (for  $F_0 \approx 5 \times 10^{-3}$ ) making the experimental resolution of the spectrum feasible.

We are grateful to Felix Izrailev for the permission to use his code for his NNS distribution. Support of KBN under Project No. 2P302B-00915 (K.S. and J.Z.) is acknowledged. This work is a part of the Alexander von Humboldt scholarship proposal (K.S.). Laboratoire Kastler Brossel de l'Université Pierre et Marie Curie et de l'École Normale Supérieure is UMR 8552 du CNRS.

The additional support of the bilateral Polonium and PICS programs is appreciated.

- 
- [1] O. Bohigas, in *Chaos and Quantum Physics*, 1899 Les Houches Lecture Session LII, edited by M.-J. Giannoni, A. Voros, and J. Zinn-Justin (North-Holland, Amsterdam, 1991), p. 87.
  - [2] M. V. Berry and M. Tabor, Proc. R. Soc. London A **356**, 375 (1977); **400**, 229 (1985).
  - [3] T. A. Brody, Lett. Nuovo Cimento **7**, 482 (1973).
  - [4] F. M. Izrailev, Phys. Rep. **196**, 299 (1990); G. Casati, F. Izrailev, and L. Molinari, J. Phys. A **24**, 4755 (1991).
  - [5] M. V. Berry and M. Robnik, J. Phys. A **17**, 2413 (1984); T. Prosen and M. Robnik, J. Phys. A **26**, 2371 (1993); **27**, 8059 (1994); M. Robnik, J. Dobnikar, and T. Prosen, *chao-dyn/9711011*.
  - [6] P. So *et al.*, Phys. Rev. Lett. **74**, 2662 (1995); U. Stoffregen *et al.*, Phys. Rev. Lett. **74**, 2666 (1995).
  - [7] H. Friedrich and D. Wintgen, Phys. Rep. **183**, 37 (1989); P. M. Koch and K. A. H. van Leeuwen, Phys. Rep. **255**, 289 (1995).
  - [8] M. C. Gutzwiller, *Chaos in Classical and Quantum Mechanics* (Springer-Verlag, New York, 1990).
  - [9] J. von Milczewski, G. H. F. Diercksen, and T. Uzer, Phys. Rev. Lett. **73**, 2428 (1994); J. von Milczewski and T. Uzer, Phys. Rev. E **55**, 6540 (1997).
  - [10] J. Main, M. Schwacke, and G. Wunner, Phys. Rev. A **57**, 1149 (1998).
  - [11] C. Cohen-Tannoudji, J. Dupont-Roc, and G. Grynberg, *Atom-Photon Interaction: Basic Processes and Applications* (John Wiley and Sons, New York, 1992).
  - [12] A. Buchleitner, D. Delande, K. Sacha, and J. Zakrzewski, (unpublished).
  - [13] K. Sacha, J. Zakrzewski, and D. Delande, Eur. Phys. J. D **1**, 231 (1998); K. Sacha and J. Zakrzewski, Phys. Rev. A **58**, 3974 (1998); **59**, 1707 (1999); A. Buchleitner, K. Sacha, D. Delande, and J. Zakrzewski, Eur. Phys. J. D **5**, 145 (1999).
  - [14] A. Buchleitner and D. Delande, Phys. Rev. A **55**, R1585 (1997).
  - [15] *Handbook of Mathematical Functions*, edited by M. Abramowitz and I. A. Stegun (Dover, New York, 1972).
  - [16] K. Sacha and J. Zakrzewski, Phys. Rev. A **58**, 488 (1998).